

Molecular and Dissociative Adsorption of H₂O on ZrO₂/YSZ Surfaces



Dilshod Nematov

Abstract: The work involves first-principles calculations to study the mechanism of adsorption of water molecules on the surface of ZrO₂ and their yttrium-stabilized structures (YSZ). Calculations of the electronic properties of ZrO₂ showed that during the m-t phase transformation of ZrO₂, the Fermi level first shifts by 0.125 eV towards the conduction band, and then in the t-c region goes down by 0.08 eV. In this case, the band gaps for c-ZrO₂, t-ZrO₂ and m-ZrO₂, respectively, are 5.140 eV, 5.898 eV and 5.288 eV. Calculations to determine the surface energy showed that t-ZrO₂ (101) and m-ZrO₂ (111) have the most stable structure, on the basis of which it was first discovered that the surface energy is somehow inversely related to the value of the band gap, since as the band gap increases, the surface energy tends to decrease. An analysis of the mechanism of water adsorption on the surface of t-ZrO₂ (101) and t-YSZ (101) showed that H₂O on unstabilized t-ZrO₂ (101) is adsorbed dissociatively with an energy of -1.22 eV, as well as by the method of molecular chemisorption with an energy of -0.69 eV and the formation of a hydrogen bond with a bond length of 1.01 Å. In the case of t-YSZ (101), water is molecularly adsorbed onto the surface with an energy of -1.84 eV. Dissociative adsorption of water occurs at an energy of -1.23 eV, near the yttrium atom. The obtained results complement the database of research works carried out in the field of the application of biocompatible zirconium dioxide crystals and ceramics in green energy generation, and can be used in designing humidity-to-electricity converters and in creating solid oxide fuel cells based on ZrO₂.

Keywords: Zirconium Dioxide, Stability, Yttrium-Stabilized Zirconium Dioxide, Phase Transition, Fermi Level Shift, Water Adsorption on The Surface.

I. INTRODUCTION

Solid-state materials based on zirconia have been extensively studied in recent years because of their excellent electrical, optical, and mechanical properties. They are also biocompatible and have a wide range of biomedical applications. Tetragonal phase yttrium-stabilized zirconia (Y-TZP) has been used in various medical applications since the 1980s, particularly for dental crowns [1]. In addition, bulk materials and nanocomposites based on ZrO₂ are used in electrochemical cells because of their high oxide ion conductivity and catalytic activity, low thermal conductivity, mechanical/chemical stability, and compatibility with electrolytes, which make them structurally advantageous [2,3]. Many technological applications of zirconia (pure ZrO₂ or its stabilized alloys) are directly related to its interaction with water.

Manuscript received on 23 November 2023 | Revised Manuscript received on 07 October 2023 | Manuscript Accepted on 15 October 2023 | Manuscript published on 30 October 2023.

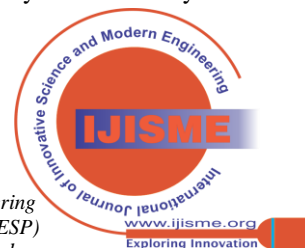
*Correspondence Author(s)

Dilshod Nematov*, S.U. Umarov Physical-Technical Institute of NAST, 734042 Tajikistan. E-mail: dilnem@mail.ru, ORCID ID: [0000-0001-6987-584X](https://orcid.org/0000-0001-6987-584X)

© The Authors. Published by Blue Eyes Intelligence Engineering and Sciences Publication (BEIESP). This is an open access article under the CC-BY-NC-ND license <http://creativecommons.org/licenses/by-nc-nd/4.0/>

Examples are internal steam reforming in solid oxide fuel cells [4], catalysis [5], gas sensors [6], or its use as a biocompatible material [7]. ZrO₂ surfaces have also been proposed as suitable materials for hydrogen storage [4–8]. However, little is known about the interaction of water with ZrO₂ surfaces at a fundamental level, which is mainly due to the lack of suitable samples. This is quite different for other oxide substrates [8–10]. Water is weakly adsorbed by many defect-free oxide surfaces in an ultra-high vacuum, then stripped at a temperature below room temperature. Usually, at 160–250 K [11], water can bind more strongly to surfaces with defects, as was shown for rutile (TiO₂ (110)) [12]. In these cases, H₂O dissociates into an OH group, which fills the oxygen vacancy, and into a hydrogen atom, which binds to surface oxygen and forms a second OH group. These OH groups are stable for up to 490 K on TiO₂ [13]. On a defect-free surface oxides (e.g., α-Cr₂O₃ (001) [14], α-Fe₂O₃ (012) [15], and oxides of alkaline earth metals, including Ca₃Ru₂O₇ (001) [16]), water can be strongly bound if the end of the surface includes highly active cations. Then, it can easily dissociate. On the surfaces of RuO₂ (110), PdO (101), and Fe₃O₄ (001), water binds coordinatively unsaturated cations and partially dissociated forms of the structure stabilized by hydrogen bonds [17–19]. High-enthalpy adsorption of low-H₂O powder materials (≥2 eV on monoclinic and ≈1.5 eV on tetragonal ZrO₂) has been reported to decrease liquid–water binding (0.45 eV) at coverages of approximately 2–4 H₂O/nm² [20][53]. In another study, Droshekevich et al [21], reported on the chemo-electronic conversion of water adsorption energy into electricity on the surface of zirconium dioxide nanopowders that were synthesized at sizes of 7.5 nm, when doped with 3 mol. % Y₂O₃.

However, despite numerous studies in this area, water adsorption on ZrO₂ surfaces has not been studied in detail, and only a few reports on H₂O adsorption can be found in the literature. In particular, H₂O adsorption on well-defined monoclinic surfaces of zirconia (m-ZrO₂ (101) and m-ZrO₂ (101) and its doped structures) has not been studied. For example, it is especially difficult to experimentally study pure ZrO₂ single crystals grown from a melt; they exhibit phase transformations upon cooling; therefore, their doped structures (e.g., YSZ) are usually investigated. However, the surface chemistry of YSZ is more complex than pure ZrO₂, as shown for CO and CO₂ adsorption [22]. In another work, Kobayashi et al [23], found that YSZ slowly decomposed at about 250 °C due to the t–m transformation. In a humid atmosphere, this t–m transformation is accompanied by microcracks and a loss in material strength. This discovery cooled the excitement caused by the discovery of PPT in zirconia-based ceramics.



This t–m transformation due to the presence of water or a humid environment in zirconia-based ceramic materials has been termed low-temperature degradation, or aging of ZrO₂ crystals. This topic has been researched extensively over the past couple of decades, including many hypotheses and discussions. The most reliable hypothesis about YSZ is based on filling oxygen vacancies present in the matrix to maintain a stable t-YSZ phase. Thus, the filling of these O vacancies with water radicals, either O₂ or OH, destabilizes the t-YSZ phase. However, the YSZ stabilization mechanism has not been fully studied, and is still the subject of numerous discussions. Therefore, the theoretical study and modeling of water adsorption on these surfaces is necessary as a starting point for a good understanding of ongoing processes and phenomena from a fundamental point of view. On the other hand, aspects of the shift in the Fermi level after doping with yttrium oxide in ZrO₂, as well as when it is under the influence of water adsorption, are still not clear due to the difficulty of their detection. For these reasons, to obtain detailed information on the process of the adsorption of water molecules onto ZrO₂ and YSZ surfaces, as well as the effect of doping on their electronic and structural properties, we conducted quantum chemical calculations within the framework of density functional theory (DFT).

II. MATERIALS AND RESEARCH METHODS

The choice of the adsorbed surface is very important for studying the interaction of water with the surface of solids, and in order to obtain accurate results, it is necessary to select a plate with the lowest density of surface broken bonds and electrostatic repulsion of neighboring layers, taking into account the thermodynamic stability of this surface. The higher the surface energy, the more thermodynamically unstable it is [24] and the more difficult it is to create an appropriate surface, namely, the surface energy is closely related to the number of atoms in the surface structure and the depth of the vacuum layer. In this work, in order to select the appropriate optimal surface for water adsorption and study its behavior on this surface, we determine the surface energy (σ) from the following equation:

$$\sigma = \frac{1}{2} \frac{[E_{slab} - (N/n)E_{bulk}]}{S} \quad (1)$$

where S is the total surface area of the plate; E_{slab} is the total plate energy; E_{bulk} is the total energy of an optimized bulk structure; N and n represent the total numbers of atoms in the surface structure and unit cell, respectively; and 2 represents the two surfaces of the calculated structure in the direction of the z -axis. Crystalline slab surface models were built based on an extended 2×2 supercell with a large vacuum space of 35 Å along the Z direction to minimize interactions between adjacent layers. Taking into account the accuracy and time of calculation, the lower layers of the surface slab were frozen, and the upper part was allowed to relax. Calculations were carried out based on density functional theory [25] using the Vienna Ab-initio Simulation Package (VASP 6.3.2) [26]. The total energy was determined using the exchange–correlation potential GGA. A $3 \times 3 \times 1$ k-point grid using the Monkhorst-Pack scheme was used to calculate a 2×2 slab. Then, each molecule in the gas phase was placed in a large box with

dimensions $11 \times 13 \times 10$ Å to avoid lateral interactions. Single H₂O molecules were initially positioned at a height of 2.5 Å above the selected surface, and different orientations were compared for each initial adsorption site, relaxing the H₂O molecules along with the top layers of the slab (Figure 1a, d). Four initial adsorption sites were tested for each molecule (on top of the Zr atom, above the outermost oxygen Ou (up), Od (down), and also centrally above the Zr position (Figure 1b). For the YSZ surface model, different initial sites were also tested adsorption sites: above the Zr atom, the outermost oxygen Ou (up), Od (down), in the position of the oxygen vacancy, above the yttrium atom and the center of the Ou–Od–Zr bonds (see Figure 1c) to find the most favorable adsorption sites, leading to stable configurations. Nonequivalent initial adsorption sites were not further studied. Oxygen vacancies were specified and taken into account by removing one O atom for each subsequent replacement of 2 Y³⁺ ions at the Zr⁴⁺ site. In this case, H (1^s), O (2^s, 2^p), Zr (4^d, 5^s) and Y (4^s 4^p 4^d 5^s) were treated as valence electrons, while the remaining electrons remained frozen. The kinetic energy cutoff was fixed at 600 eV, and all calculations were carried out taking spin-polarized effects into account.

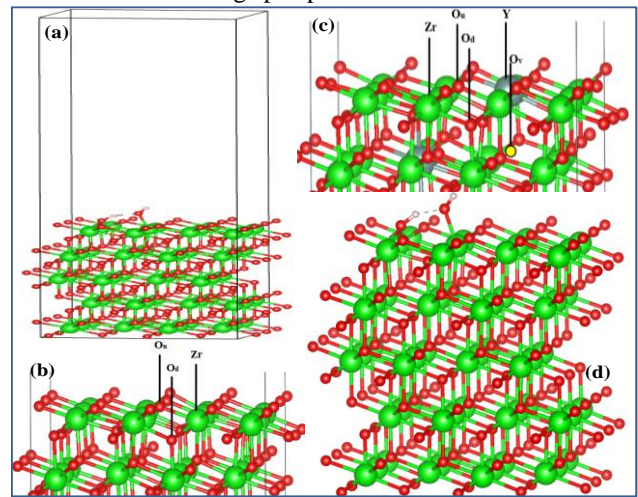


Figure 1. Optimized structures of (a) t-ZrO₂ (101) and with H₂O molecule in a box with a vacuum of 35 Å, (b) possible sites for H₂O adsorption on the surface of t-ZrO₂ (101), (c) initial sites of H₂O adsorption on the surface t-YSZ (101) and (d) model of dissociative adsorption of water on t-ZrO₂ (101).

The energy of water adsorption (E_{ads}) was determined by the following equation:

$$E_{ads} = E_{H_2O+surface} - (E_{surface} + E_{H_2O}) \quad (2)$$

To take into account long-range uncoupled interactions, we considered Van der Waals effects as the difference between the calculated Van der Waals energy of a plate with adsorbed H₂O molecules ($E_{H_2O/surface}^{vdW}$) and the sum of the calculated Van der Waals energies of the surface ($E_{surface}^{vdW}$) and H₂O molecules ($E_{H_2O}^{vdW}$):

$$E_{ads}^{vdW} = E_{H_2O/surface}^{vdW} - (E_{surface}^{vdW} + E_{H_2O}^{vdW}) \quad (3)$$

where the interaction energy vdW is taken into account by the Leonard–Jones potential.

III. RESULTS AND DISCUSSION

At the first stage of modeling, geometric optimization of the monoclinic, tetragonal and cubic phases of ZrO_2 was carried out using the VASP package. To get a good optimized structure, we applied the SCAN functionality, which is well recommended in this matter [27], to evaluate the exchange-correlation effects in the system. The optimal k-dot numbers ($4 \times 4 \times 4$) and cutoff energy (ENCUT = 600 eV) were established after several rounds of convergence testing. According to the results obtained, the lattice parameters of the monoclinic phase of zirconium dioxide ($a=5.115 \text{ \AA}$, $b=5.239 \text{ \AA}$, $c=5.304 \text{ \AA}$; $\beta=99.110^\circ$) are in good agreement with experimental data [28]. Similar results were also obtained for the tetragonal ($a=b=3.622 \text{ \AA}$, $c=5.275 \text{ \AA}$; $c/a=1.456 \text{ \AA}$, $dz=0.013$) and cubic phase ($a=b=c=5.12 \text{ \AA}$), which are in fairly good agreement with experimental results of independent authors [29-32]. Figure 2 (a-c) compares the X-ray diffraction peaks with literature counterparts, from which it can be seen that our results are in good agreement with the experimental data, with the exception of an imperceptible difference in the position of the X-ray peaks for the tetragonal system.

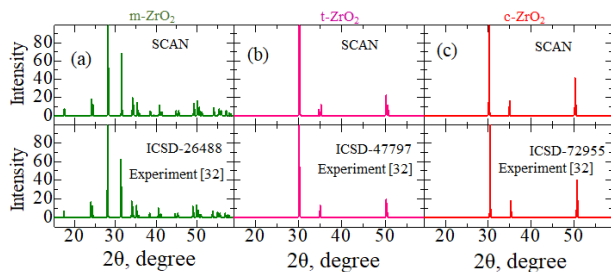


Figure 2. Comparison of experimental and calculated (SCAN) X-ray diffraction patterns of m-ZrO₂ (a), t-ZrO₂ (b), and c-ZrO₂ (c).

Based on these relaxed structures, we carried out calculations to study the electronic properties of c-ZrO₂, t-ZrO₂, m-ZrO₂. Figure 3 (a-c) shows the results of calculations of the density of states, which are crucial for the interpretation of the electronic properties of ZrO_2 , as well as the characteristics of devices based on them. To avoid underestimating the energy gap, we used the hybrid functional HSE06 [33].

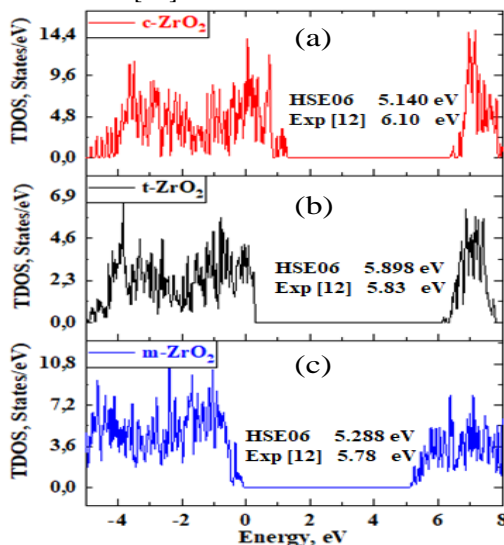


Figure 3. Total density of electronic states for c-ZrO₂ (a), t-ZrO₂ (b), and m-ZrO₂ (c).

According to Figure 3, the density of states of c-ZrO₂ is slightly higher compared to other phases. It can be seen that among the studied modifications of zirconium dioxide, the tetragonal phase has the largest band gap. Changes in the energy gap value depending on the phase can be observed from the energy diagram shown in the Figure 4.

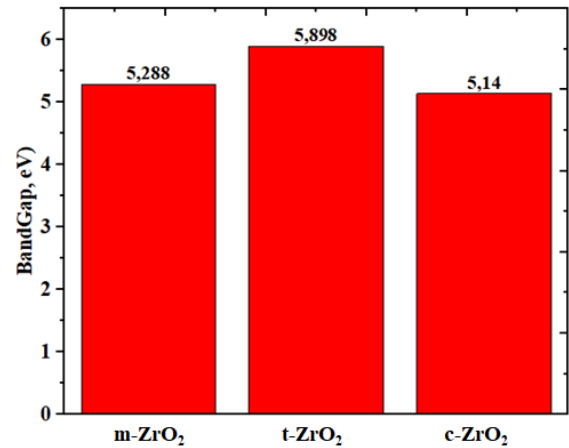


Figure 4. Diagram of the Band Gap Depending on the Phase Modification of ZrO₂.

Using the position of the Fermi level (maximum of the valence band) for the monoclinic phase as a reporting point, we estimated the shift of the Fermi level during the phase transformation of ZrO_2 . According to the results, in the m-t region the Fermi level first shifts by 0.125 eV towards the valence band, and then in the t-c region it decreases by 0.08 eV.

Next, to select the optimal adsorbed surface, we created different surface models using well-reacted unit cells of monoclinic, tetragonal and cubic ZrO_2 to correctly calculate the surface energy (σ) for slightly different surface models with different Miller indices. The surface energy values for various ZrO_2 slab models are calculated using formula 1 and are shown in Table 1. These steps were implemented based on the fact that choosing a slab with the lowest surface energy is an important task in order to correctly model the phenomena of water adsorption on the corresponding surface.

Table 1. Calculated Values of Surface Energies (σ) for the Main Types of ZrO₂ plate.

Phase	Miller Indices	$\sigma, 10^{19} \text{ eV/m}^2$
m-ZrO ₂	-1	1.54
	-10	1.16
	-110	1.1
	-101	1.23
	-11	1.08
t-ZrO ₂	-111	0.81
	-1	0.98
	-10	0.95
c-ZrO ₂	-101	0.78
	-100	1.01
	-111	0.79
	-100	1.51
	-110	1.34
	-111	1.12

According to the results presented in Table 1, it can be seen that the most stable surfaces are those of the tetragonal and monoclinic phases, namely t-ZrO₂ (101) and m-ZrO₂ (111). Based on the results obtained, it can be assumed that the surface energy is somehow related to the size of the band gap, since with an increase in the band gap, the surface energy tends to decrease. That is, the results obtained demonstrate an inverse relationship between the surface energy and the results shown in the band gap diagram (Fig. 4). The results obtained are consistent with the work of Maliki et al [34], which reported that the most stable surface can be obtained from t-ZrO₂ (101). As for comparing the results to experimental data, there are no reported data in the literature because the surface energies of solid metal oxides are difficult to measure experimentally. In total, measurements of the surface energies of some types of zirconium dioxide surfaces using multiphase balancing at high temperatures has been reported [35]. Based on the results obtained, we chose the t-ZrO₂ (101) surface for this study, as the most stable surface for water molecule adsorption. After final surface preparation, single H₂O molecules were initially positioned 2.5 Å above the selected surface with different orientations, which is larger than the bond distance between Zr and O (2.12 Å) in the solid state. The structures were then optimized by freezing the bottom layers of the wafer (Figure 5(a)).

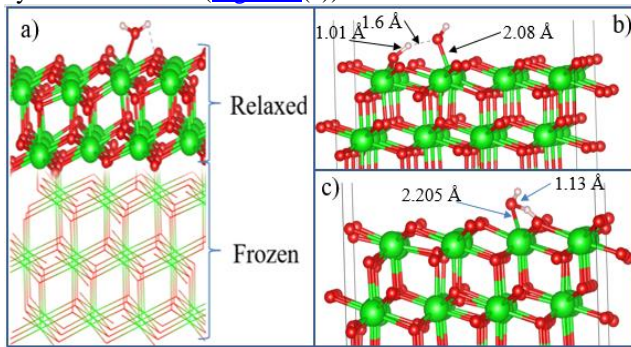


Figure 5. Configuration of water molecule adsorption on the surface of t-ZrO₂ (101): (a) model of a lamellar t-ZrO₂ (101) cell with the initial configuration of water on its surface, (b) dissociative adsorption in a side view, (c) model of molecular physisorption of water on the surface of t-ZrO₂ in a side view.

The optimized structure of the H₂O/t-ZrO₂ (101) system is shown in Figure 5 (b), from which it can be seen that the H₂O molecule is dissociatively adsorbed with an energy of -1.221 eV, even in the most favorable region (where the system has a minimum energy stable configuration). Dissociative adsorption of water on ZrO₂ was also observed in the work of Korhonen et al. [36], where they experimentally and theoretically proved that water at low coverage dissociates on the surface of m-ZrO₂, and our calculated adsorption energy on t-ZrO₂ (101) for [H+OH]-ZrO₂(101) is similar to that obtained by these authors results (E_{ads}=1.20 eV) for (111) from the monoclinic phase. It was also found that at a given surface, water is adsorbed by molecular chemisorption, in which the oxygen of the water molecule coordinates the surface cation, and a small extension of one O–H water bond (1.13 Å) occurs in the form of hydrogen bonds of water with

the surface oxygen ion (Figure 5 (c)). In this case, the adsorption energy is equal to 0.69 eV, and the distance between the oxygen of the water molecule and the zirconium atom of the surface is 2.205 Å. At the same time, the proton (H) in the water molecule and the oxygen from the surface of the slab form a hydrogen bond with a bond length of 1.01 Å. Next, to study the mechanism of water adsorption on the t-YSZ surface, we replaced two Zr (from the topmost and subsurface O-Zr-O trilayers with Y, removing one oxygen from the third atomic layer (the next nearest neighbor of the Y atoms) to obtain a surface like t-YSZ (101). As the results showed, the water molecule is molecularly adsorbed and also dissociated on the surface of t-YSZ (101). Molecular adsorption of water at the most optimal configuration occurs with an energy of -1.84 eV, and the bond length of water from the surface t-YSZ (101) increases to 2.73 Å (Figure 6 (a)), while the O-H distance in water molecules remains unchanged.

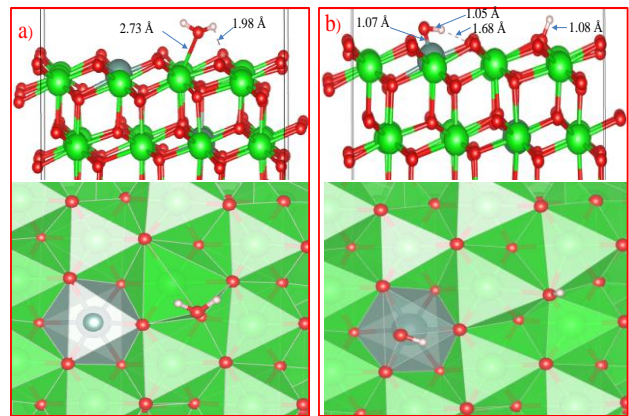


Figure 6. Molecular (a) and Dissociated Adsorption of Water to Form Surface Hydroxyls (b) in the H₂O-YSZ (101) Model.

Dissociative adsorption of water was accompanied by the movement of oxygen in the vacancy region of the plate, which leads to very strong adsorption with an energy of -1.23 eV, blocking surface areas for oxygen activation. In both cases, H₂O is adsorbed close to the yttrium atom (Figure 6(b)). Unlike adsorption on t-ZrO₂(101), water is more stably adsorbed on t-YSZ(101), since the adsorption energy of H₂O-YSZ(101) is more favorable than that of (H+OH)-YSZ(101). Comparative analysis of the electronic structure of the H₂O-ZrO₂(101) and H₂O-YSZ (101) systems indicates that the H₂O interaction almost does not change the configuration of the electronic properties in the system (except for increasing the density state) when the system is modified with Y impurities (Figure 7). However, water molecules preferentially tend to adsorb molecularly on the t-YSZ(101) surface, whereas on t-ZrO₂(101) it preferentially adsorbs dissociatively. Table 2 summarizes some of the main data obtained from the simulation of water adsorption on t-ZrO₂(101) and t-YSZ surfaces.

Table 2. Adsorption Energies (Eads) and Geometric Characteristics of t-ZrO₂(101) and t-YSZ (101) with Adsorbed Water

	t-ZrO ₂ (101)	t-YSZ (101)
Eads (H ₂ O), eV	-	- 1.84
Eads (H+OH), eV	- 1.22	- 1.23
Dist O(H ₂ O)-surf, Å	2.08	2.73
Dist O(H ₂ O)-H1(H ₂ O), Å	0.97	0.96
Dist O(H ₂ O)-H2(H ₂ O), Å	1.13	0.97
H-O-H bond angle, (°)	111.3	105.54

Doping with Y₂O₃ stabilizes t-ZrO₂(101) and is accompanied by greater relaxation of O atoms. Calculations of the electronic properties of the H₂O-ZrO₂ (101) and H₂O-YSZ (101) systems were carried out using the GGA functional, since the computing power of our computer was insufficient to implement the calculations with sewing functionality HSE06. However, the results of calculations using the GGA functional greatly underestimate the band gap of the system (3.24 eV for the H₂O-ZrO₂ (101) system and 3.21 eV for H₂O-YSZ (101)). On the other hand, it was revealed that due to the presence of O-th vacancies, no new interband energy states are formed in the t-YSZ band diagram (Figure 7).

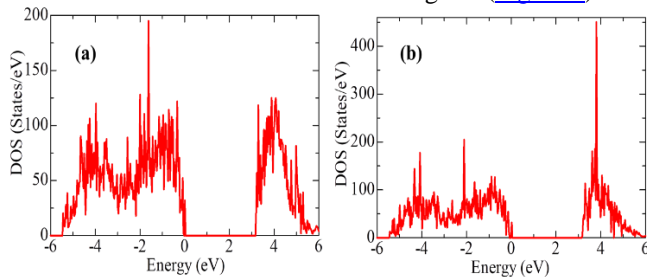


Figure 7. GGA-Calculated Total Density of states for (a) t-ZrO₂ (101) and (b) t-YSZ (101) Upon Interaction with Water Molecules.

It is also important to take into account the hydrophilic nature of ZrO₂ in such studies. Research shows that in addition to physically adsorbed water, there are terminal, bi-bridging and triple-bridging OH groups on the surface of the substrate, which are actively involved in the surface reaction [37-50][51][52]. Surface hydroxyl groups and H₂O adsorbed on the surface can partially block the active sites (lattice oxygen ions on the surface) of YSZ oxidation. The fully hydroxylated model t-YSZ (101) surface configuration is shown in Figure 8(a). The results show that the OH groups form strong bonds from the slab surface. Figure 8 (b) shows the adsorption structure of a single water molecule on a fully hydroxylated YSZ surface.

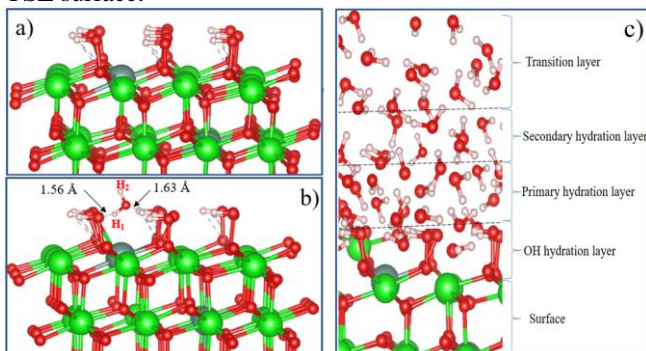


Figure 8. Relaxed Configurations: (a) Fully Hydroxylated t-YSZ (101), (b) Single Water Adsorptions on the fully Hydroxylated t-YSZ (101) Surface, and (c) Hydration Model of the t-YSZ (101) Surface.

It can be seen that the repulsive forces of oxygen and hydrogen atoms in a water molecule and OH atoms on a completely hydroxylated surface do not prevent the H₂O molecule from being adsorbed on t-YSZ (101). When water is adsorbed, two strong hydrogen bonds are formed on the hydroxylated surface, distances of 1.56 and 1.63 Å. In this case, water is adsorbed with an adsorption energy of 0.34 eV. The single water molecule adsorption model and other similar systems will help in the future to study in detail more complex models, including the multilayer hydration structure of the interface (Figure 8). Although this model requires a lot of computing power for DFT calculations, it can be assumed that in the layer closest to the surface (hydroxyl hydration layer), most water molecules can be adsorbed dissociatively. Further, through hydrogen bonding, H₂O molecules will continue to be adsorbed and regularly located on the hydroxylated surface, forming primary and secondary hydration layers. The regularity of H₂O molecules in the outer layer can be considered as a transition layer, and the hydration structure of the first three layers of H₂O located near the surface can be considered as a group of water molecules that can be stably adsorbed and exist on the t-YSZ (101) surface. However, a detailed study of the full hydration model of the t-YSZ (101) surface remains the subject of our future studies.

IV. CONCLUSIONS

The processes of H₂O adsorption on the surface of t-ZrO₂ (101) and t-YSZ (101) were studied using quantum chemical calculations. Calculations showed that H₂O on unstabilized t-ZrO₂ (101) is adsorbed dissociatively with an energy of 1.22 eV. Also on this surface, water is adsorbed by molecular chemisorption with an energy of -0.69 eV and the formation of a hydrogen bond with a bond length of 1.01 Å. In the case of t-YSZ (101), water is molecularly adsorbed on the surface with an energy of -1.84 eV. Dissociative adsorption of water occurs with an energy of 1.23 eV near the yttrium atom. This research will help in the future to build a more accurate computational model for detailed studies of materials such as YSZ.

DECLARATION STATEMENT

Funding/ Grants/ Financial Support	The research leading to these results has received funding from the European Union's Horizon 2020 research and innovation programme under the Marie Skłodowska-Curie grant agreement 871284 project SSHARE.
Conflicts of interest	No conflicts of interest to the best of our knowledge.
Ethical Approval and Consent to Participate	No, this article does not require ethical approval and consent to participate with evidence.
Availability of Data and Material/ Data Access Statement	Not relevant.
Authors Contributions	I am only the sole author of the article

REFERENCES

- Chevalier, J.; Gremillard, L.; Deville, S. Low-Temperature Degradation of Zirconia and Implications for Biomedical Implants. *Annu. Rev. Mater. Res.* 2007, 37, 1–32. <https://doi.org/10.1146/annurev.matsci.37.052506.084250>.
- Nikumbh, A.K.; Adhyapak, P.V. Formation characterization and rheological properties of zirconia and ce-ria-stabilized zirconia. *Nat. Sci.* 2010, 2, 694.
- Lee, W.E.; Rainforth, M. *Ceramic Microstructures: Property Control by Processing*; Springer Science & Business Media: Berlin/Heidelberg, Germany, 1994; p. 317.
- Hecht, E.S.; Gupta, G.K.; Zhu, H.; Dean, A.M.; Kee, R.J.; Maier, L.; Deutschmann, O. Methane reforming kinetics within a Ni–YSZ SOFC anode support. *Appl. Catal. A: Gen.* 2005, 295, 40–51. <https://doi.org/10.1016/j.apcata.2005.08.003>.
- Tanabe, K. Surface and catalytic properties of ZrO₂. *Mater. Chem. Phys.* 1985, 13, 347–364. [https://doi.org/10.1016/0254-0584\(85\)90064-1](https://doi.org/10.1016/0254-0584(85)90064-1).
- Liu, Y.; Parisi, J.; Sun, X.; Lei, Y. Solid-state gas sensors for high temperature applications—A review. *J. Mater. Chem. A* 2014, 2, 9919–9943. <https://doi.org/10.1039/c3ta15008a>.
- Hisbergues, M.; Vendeville, S.; Vendeville, P. Zirconia, Established facts and perspectives for a biomaterial in dental im-plantology. *J. Biomed. Mater. Res. Part B* 2009, 88, 519–529.
- Henderson, M.A. The interaction of water with solid surfaces: Fundamental aspects revisited. *Surf. Sci. Rep.* 2002, 46, 1–308. [https://doi.org/10.1016/s0167-5729\(01\)00020-6](https://doi.org/10.1016/s0167-5729(01)00020-6).
- Mu, R.; Zhao, Z.-J.; Dohnálek, Z.; Gong, J. Structural motifs of water on metal oxide surfaces. *Chem. Soc. Rev.* 2017, 46, 1785–1806. <https://doi.org/10.1039/c6cs00864j>.
- Nematov, D.D.; Kholmurodov, K.T.; Husenzoda, M.A.; Lyubchik, A.; Burhonzoda, A.S. Molecular Adsorption of H₂O on TiO₂ and TiO₂: Y Surfaces. *J. Hum. Earth Futur.* 2022, 3, 213–222. <https://doi.org/10.28991/hef-2022-03-02-07>.
- Campbell, C.T.; Sellers, J.R.V. Enthalpies and Entropies of Adsorption on Well-Defined Oxide Surfaces: Experimental Measurements. *Chem. Rev.* 2013, 113, 4106–4135. <https://doi.org/10.1021/cr300329s>.
- Zhang, Z.; Bondarchuk, O.; Kay, B.D.; White, J.M.; Dohnálek, Z. Imaging Water Dissociation on TiO₂(110): Evidence for Inequivalent Geminate OH Groups. *J. Phys. Chem. B* 2006, 110, 21840–21845. <https://doi.org/10.1021/jp063619h>.
- Henderson, M.A. Structural Sensitivity in the Dissociation of Water on TiO₂ Single-Crystal Surfaces. *Langmuir* 1996, 12, 5093–5098. <https://doi.org/10.1021/la960360t>.
- Henderson, M.A.; Chambers, S.A. HREELS, TPD and XPS study of the interaction of water with the α -Cr₂O₃ (001) surface. *Surf. Sci.* 2000, 449, 135–150.
- Henderson, M.A.; Joyce, S.A.; Rustad, J.R. Interaction of water with the (1 × 1) and (2 × 1) surfaces of α -Fe₂O₃ (012). *Surf. Sci.* 1998, 417, 66–81.
- Hu, X.L.; Carrasco, J.; Klimeš, J.; Michaelides, A. Trends in water monomer adsorption and dissociation on flat insulating surfaces. *Phys. Chem. Chem. Phys.* 2011, 13, 12447–12453. <https://doi.org/10.1039/c1cp20846b>.
- Lobo, A.; Conrad, H. Interaction of H₂O with the RuO₂(110) surface studied by HREELS and TDS. *Surf. Sci.* 2003, 523, 279–286. [https://doi.org/10.1016/s0039-6028\(02\)02459-7](https://doi.org/10.1016/s0039-6028(02)02459-7).
- Kan, H.H.; Colmyer, R.J.; Asthagiri, A.; Weaver, J.F. Adsorption of water on a PdO (101) thin film: Evidence of an adsorbed HO–H₂O complex. *J. Phys. Chem. C* 2009, 113, 1495–1506.
- Meier, M.; Hulva, J.; Jakub, Z.; Pavelec, J.; Setvin, M.; Bliem, R.; Schmid, M.; Diebold, U.; Franchini, C.; Parkinson, G.S. Water agglomerates on Fe₃O₄ (001). *Proc. Natl. Acad. Sci. USA* 2018, 115, E5642–E5650.
- Radha, A.V.; Bomati-Miguel, O.; Ushakov, S.V.; Navrotsky, A.; Tartaj, P. Surface enthalpy, enthalpy of water adsorption, and phase stability in nanocrystalline monoclinic zirconia. *J. Am. Ceram. Soc.* 2009, 92, 133–140.
- Doroshkevich, A.S.; Asgerov, E.B.; Shylo, A.V.; Lyubchik, A.I.; Logunov, A.I.; Glazunova, V.A.; Islamov, A.K.; Turchenko, V.A.; Almasan, V.; Lazar, D.; et al. Direct conversion of the water adsorption energy to electricity on the surface of zirconia nanoparticles. *Appl. Nanosci.* 2019, 9, 1603–1609. <https://doi.org/10.1007/s13204-019-00979-6>.
- Kock, E.M.; Kogler, M. In situ FT-IR spectroscopic study of CO₂ and CO adsorption on Y₂O₃, ZrO₂, and yttria-stabilized ZrO₂. *J. Phys. Chem. C* 2013, 117, 17666–17673.
- Kobayashi, K.; Kuwajima, H.; Masaki, T. Phase change and mechanical properties of ZrO₂-Y₂O₃ solid electrolyte after ageing. *Solid State Ion.* 1981, 3–4, 489–493. [https://doi.org/10.1016/0167-2738\(81\)90138-7](https://doi.org/10.1016/0167-2738(81)90138-7).
- Liu, J., Gong, G., Han, Y., & Zhu, Y. (2017). New insights into the adsorption of oleate on cassiterite: A DFT study. *Minerals*, 7(12), 236.
- Hohenberg, P., & Kohn, W. (1964). Inhomogeneous electron gas. *Physical review*, 136(3B), B864.
- Kresse G, Furthmuller J. Efficiency of ab-initio total energy calculations for metals and semiconductors using a plane-wave basis set. *Comput. Mater. Sci.* 1996; 6:15–50
- Sun, J., Ruzsinszky, A., & Perdew, J. P. (2015). Strongly constrained and appropriately normed semilocal density functional. *Physical review letters*, 115(3), 036402.
- Howard, C. J., Hill, R. J., & Reichert, B. E. (1988). Structures of ZrO₂ polymorphs at room temperature by high-resolution neutron powder diffraction. *Acta Crystallographica Section B: Structural Science*, 44(2), 116-120
- Teufer, G. (1962). The crystal structure of tetragonal ZrO₂. *Acta Crystallographica*, 15(11), 1187-1187.
- Martin, U., Boysen, H., & Frey, F. (1993). Neutron powder investigation of tetragonal and cubic stabilized zirconia, TZP and CSZ, at temperatures up to 1400 K. *Acta Crystallographica Section B: Structural Science*, 49(3), 403-413.
- Aldebert, P., & TRAVERSE, J. P. (1985). Structure and ionic mobility of zirconia at high temperature. *Journal of the American Ceramic Society*, 68(1), 34-40.
- Martin, U., Boysen, H., & Frey, F. (1993). Neutron powder investigation of tetragonal and cubic stabilized zirconia, TZP and CSZ, at temperatures up to 1400 K. *Acta Crystallographica Section B: Structural Science*, 49(3), 403-413.
- Verma P, Truhlar D. HLE16: A Local Kohn-Sham Gradient Approximation with Good Performance for Semiconductor Band Gaps and Molecular Excitation Energies. *J. Phys. Chem. Lett.* 2017;8:380–87. doi.org/10.1021/acs.jpclett.6b02757.
- Maleki, F., & Pacchioni, G. (2020). Characterization of acid and basic sites on zirconia surfaces and nanoparticles by adsorbed probe molecules: A theoretical study. *Topics in Catalysis*, 63, 1717-1730.
- Tsoga, A.; Nikolopoulos, P. Surface and grain-boundary energies in yttria-stabilized zirconia (YSZ-8 mol%). *J. Mater. Sci.* 1996, 31, 5409–5413. <https://doi.org/10.1007/bf01159310>.
- Korhonen, S. T., Calatayud, M., & Krause, A. O. I. (2008). Stability of hydroxylated (111) and (101) surfaces of monoclinic zirconia: A combined study by DFT and infrared spectroscopy. *The Journal of Physical Chemistry C*, 112(16), 6469-6476.
- Kim, G., Kwon, G., & Lee, H. (2021). The role of surface hydroxyl groups on a single-atomic Rh 1/ZrO₂ catalyst for direct methane oxidation. *Chemical Communications*, 57(13), 1671-1674.
- Zhu, J., van Ommen, J. G., & Lefferts, L. (2006). Effect of surface OH groups on catalytic performance of yttrium-stabilized ZrO₂ in partial oxidation of CH₄ to syngas. *Catalysis today*, 117(1-3), 163-167.
- Nematov, D. Influence of Iodine Doping on the Structural and Electronic Properties of CsSnBr₃. *Int. J. Appl. Phys.* 2022, 7, 36–47.
- Nematov, D.; Kholmurodov, K.; Yuldasheva, D.; Rakhmonov, K.; Khojakhonov, I. Ab-initio Study of Structural and Electronic Properties of Perovskite Nanocrystals of the CsSn[Br_{1-x}I_x]₃ Family. *HighTech Innov. J.* 2022, 3, 140–150.
- Davlatshoevich, N.D. Investigation Optical Properties of the Orthorhombic System CsSnBr_{3-x}I_x: Application for Solar Cells and Optoelectronic Devices. *J. Hum. Earth Futur.* 2021, 2, 404–411. <https://doi.org/10.28991/hef-2021-02-04-08>.
- Davlatshoevich, N.D.; Ashur, K.; Saidali, B.A.; Kholmirzo, K.; Lyubchik, A.; Ibrahim, M. Investigation of structural and optoelectronic properties of N-doped hexagonal phases of TiO₂ (TiO_{2-x}N_x) nanoparticles with DFT realization: Optimization of the band gap and optical properties for visible-light absorption and photovoltaic applications. *Biointerface Res. Appl. Chem.* 2022, 12, 3836–3848.
- Nematov, D.D.; Burhonzoda, A.S.; Khuseinov, M.A.; Kholmurodov, K.T.; Yamamoto, T. First Principles Analysis of Crystal Structure, Electronic and Optical Properties of CsSn13-xBrx Perovskite for Photoelectric Applications. *J. Surf. Investig. X-ray Synchrotron Neutron Tech.* 2021, 15, 532–536. <https://doi.org/10.1134/s1027451021030149>.

44. Nematov, D.D.; Kholmurodov, K.T.; Aliona, S.; Faizulloev, K.; Gnatovskaya, V.; Kudzoev, T. A DFT Study of Structure, Elec-tronic and Optical Properties of Se-Doped Kesterite Cu₂ZnSnS₄ (CZTSSe). *Lett. Appl. NanoBioSci.* 2022, 12, 67.
45. Nematov, D.; Makhudov, B.; Kholmurodov, K.; Yarov, M. Optimization Optoelectronic Properties ZnxCd1-xTe System for Solar Cell Application: Theoretical and Experimental Study. *Biointerface Res. Appl. Chem.* 2023, 13, 90.
46. Nematov, D.; Burhonzoda, A.; Khuseinov, M.; Kholmurodov, K.; Doroshkevych, A.; Doroshkevych, N.; Zelenyak, T.; Majumder, S.; Ibrahim, M. Molecular Dynamics Simulations of the DNA Radiation Damage and Conformation Behavior on a Zirconium Dioxide Surface. *Egypt. J. Chem.* 2019, 62, 12–14. <https://doi.org/10.21608/ejchem.2019.12981.1811>.
47. Nematov, D.D.; Burhonzoda, A.S.; Khuseinov, M.A.; Kholmurodov, K.T.; Ibrahim, M.A. The Quantum-Chemistry Calculations of Electronic Structure of Boron Nitride Nanocrystals with Density Functional Theory Realization. *Egypt. J. Chem.* 2019, 62, 11–12. <https://doi.org/10.21608/ejchem.2019.12879.1805>.
48. Nizomov, Z.; Asozoda, M.; Nematov, D. Characteristics of Nanoparticles in Aqueous Solutions of Acetates and Sulfates of Single and Doubly Charged Cations. *Arab. J. Sci. Eng.* 2022, 48, 867–873. <https://doi.org/10.1007/s13369-022-07128-2>.
49. Dilshod, N.; Kholmirzo, K.; Aliona, S.; Kahramon, F.; Viktoriya, G.; Tamerlan, K. On the Optical Properties of the Cu₂ZnSn[S1-xSex]₄ System in the IR Range. *Trends Sci.* 2023, 20, 4058–4058. <https://doi.org/10.48048/tis.2023.4058>.
50. Danilenko, I.; Gorban, O.; Maksimchuk, P.; Viagin, O.; Malyukin, Y.; Gorban, S.; Volkova, G.; Glasunova, V.; Mendez-Medrano, M.G.; Colbeau-Justin, C.; et al. Photocatalytic activity of ZnO nanopowders: The role of production techniques in the formation of structural defects. *Catal. Today* 2019, 328, 99–104. <https://doi.org/10.1016/j.cattod.2019.01.021>.
51. S. S. Mydeen, M. Kottaisamy, and V. S. Vasantha*, "Photocatalytic Performances and Antibacterial Activities of Nano-Zno Derived By Cetrimide-Based Co-Precipitation Method by Varying Solvents," *International Journal of Innovative Technology and Exploring Engineering*, vol. 9, no. 2. Blue Eyes Intelligence Engineering and Sciences Engineering and Sciences Publication - BEIESP, pp. 930–938, Dec. 30, 2019. doi: 10.35940/ijitee.b7145.129219. Available: <http://dx.doi.org/10.35940/ijitee.B7145.129219>.
52. "Construction of Simulation for Adsorption Process Visualization," *International Journal of Recent Technology and Engineering*, vol. 8, no. 2S6. Blue Eyes Intelligence Engineering and Sciences Engineering and Sciences Publication - BEIESP, pp. 420–423, Sep. 16, 2019. doi: 10.35940/ijrte.b1079.0782s619. Available: <http://dx.doi.org/10.35940/ijrte.B1079.0782S619>
53. S. A. Bahadur et al., "Nanocrystalline Cuco2se4 Thin Film Counter Electrode for Dye-Sensitized Solar Cells," *International Journal of Engineering and Advanced Technology*, vol. 9, no. 1s4. Blue Eyes Intelligence Engineering and Sciences Engineering and Sciences Publication - BEIESP, pp. 370–373, Dec. 30, 2019. doi: 10.35940/ijeat.a1184.1291s419. Available: <http://dx.doi.org/10.35940/ijeat.A1184.1291S419>

AUTHOR PROFILE



Dilshod Nematov has been working at the S. U. Umarov Physical-Technical Institute of the National Academy of Sciences of Tajikistan since 2021, before that he worked as a senior lecturer in the Department of Physics at the Tajik Technical University. Currently, he is a Senior Research Fellow at the Center for Research and Use of Renewable Energy Sources of the National

Academy of Sciences of Tajikistan. He is the editor of the journal "SCI-ARTICLE" on physics, energy, nanotechnology and materials science and is on the editorial board of the journal *Trends in Sciences* (2774-0226) and *Chemistry of Inorganic Materials* (2949-7469). He received a specialist degree from the Tajik National University and then a PhD in Engineering from the Tajik Technical University, Tajikistan. He has done research, provided industry advice, and published over 60 publications in his area of expertise

Disclaimer/Publisher's Note: The statements, opinions and data contained in all publications are solely those of the individual author(s) and contributor(s) and not of the Blue Eyes Intelligence Engineering and Sciences Publication (BEIESP)/ journal and/or the editor(s). The Blue Eyes Intelligence Engineering and Sciences Publication (BEIESP) and/or the editor(s) disclaim responsibility for any injury to people or property resulting from any ideas, methods, instructions or products referred to in the content.